BIOCHEMISTRY
including biophysical chemistry & molecular biology

Article

pubs.acs.org/biochemistry

Role of Annular Lipids in the Functional Properties of Leucine Transporter LeuT Proteomicelles

Michael V. LeVine,[†] George Khelashvili,[*,†] Lei Shi,[†,‡] Matthias Quick,[§,∥] Jonathan A. Javitch,[§,∥,⊥] and Harel Weinstein[†,#]

[†]Department of Physiology and Biophysics, Weill Cornell Medical College of Cornell University (WCMC), New York, New York 10065, United States

[‡]Computational Chemistry and Molecular Biophysics Unit, National Institute on Drug Abuse-Intramural Research Program, National Institutes of Health, Baltimore, Maryland 21224, United States

[§]Department of Psychiatry and [∥]Department of Pharmacology, Columbia University College of Physicians & Surgeons, New York, New York 10032, United States

[⊥]Division of Molecular Therapeutics, New York State Psychiatric Institute, New York, New York 10032, United States

[#]HRH Prince Alwaleed Bin Talal Bin Abdulaziz Alsaud Institute for Computational Biomedicine, Weill Cornell Medical College of Cornell University, New York, New York 10065, United States

Supporting Information

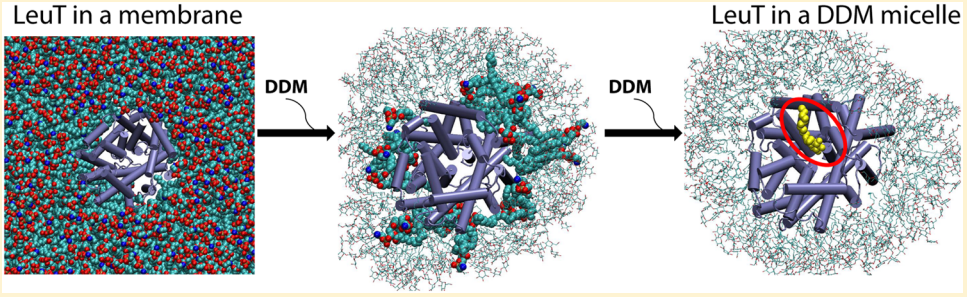

ABSTRACT: Recent work has shown that the choice of the type and concentration of detergent used for the solubilization of membrane proteins can strongly influence the results of functional experiments. In particular, the amino acid transporter LeuT can bind two substrate molecules in low concentrations of *n*-dodecyl β-D-maltopyranoside (DDM), whereas high concentrations reduce the molar binding stoichiometry to 1:1. Subsequent molecular dynamics (MD) simulations of LeuT in DDM proteomicelles revealed that DDM can penetrate to the extracellular vestibule and make stable contacts in the functionally important secondary substrate binding site (S2), suggesting a potential competitive mechanism for the reduction in binding stoichiometry. Because annular lipids can be retained during solubilization, we performed MD simulations of LeuT proteomicelles at various stages of the solubilization process. We find that at low DDM concentrations, lipids are retained around the protein and penetration of detergent into the S2 site does not occur, whereas at high concentrations, lipids are displaced and the probability of DDM binding in the S2 site is increased. This behavior is dependent on the type of detergent, however, as we find in the simulations that the detergent lauryl maltose-neopentyl glycol, which is approximately twice the size of DDM and structurally more closely resembles lipids, does not penetrate the protein even at very high concentrations. We present functional studies that confirm the computational findings, emphasizing the need for careful consideration of experimental conditions, and for cautious interpretation of data in gathering mechanistic information about membrane proteins.

Protein solubilization is a critical preparatory step in any *in vitro* experiment on membrane proteins.[1] During this process, the proteins, typically overexpressed in cells, undergo detergent-mediated extraction from the native lipid membrane environment into detergent micellar envelopes (proteomicelles).[1] Detergents with relatively large polar headgroups and short hydrophobic tails, present in the protein solution above their respective critical concentration (CMC), would solubilize a membrane protein by packing their hydrophobic tails around each other and around the protein's hydrophobic transmembrane (TM) domain, while exposing their polar headgroups to the aqueous solvent.[2] In this manner, proteomicelles effectively protect the hydrophobic TM domain from unfavorable polar exposure, while allowing hydrophilic loop regions to be directly exposed to water.

The solubilization process delicately aims to retain the full functionality of a membrane protein while creating a solution

Received: November 23, 2015
Revised: January 25, 2016
Published: January 26, 2016

DOI: 10.1021/acs.biochem.5b01268
Biochemistry 2016, 55, 850−859

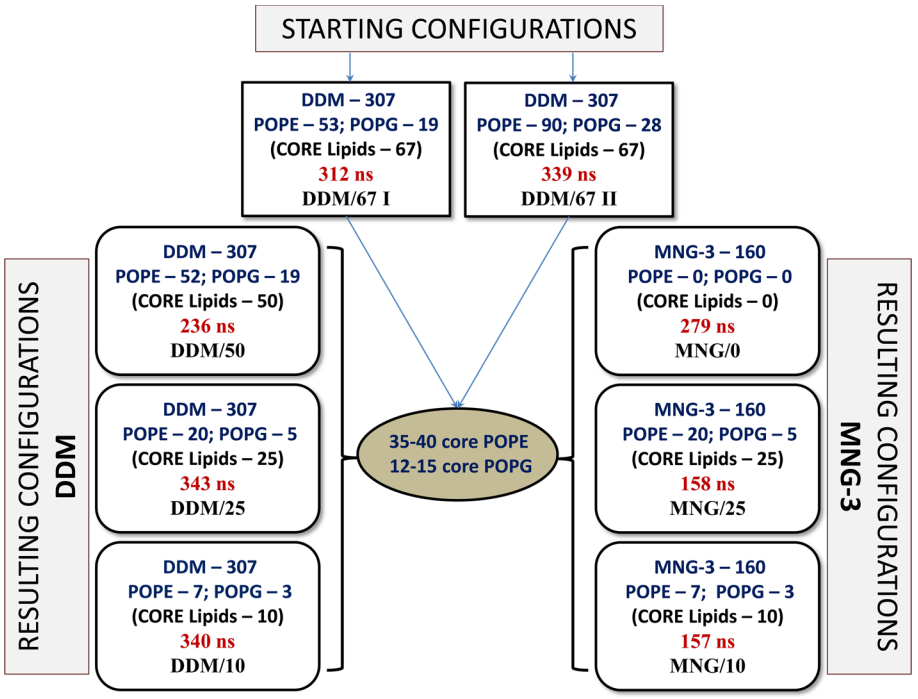

Figure 1. Schematic representation of the conditions for the all-atom MD simulations of LeuT/lipid/detergent complexes (protein:detergent:lipid number ratios and initial spatial distribution of the lipid around LeuT). DDM/67 I and DDM/67 II are simulations of the "Starting Configurations" with a lipid core consisting of a mixture of POPE and POPG phospholipids within either 5 Å (53:19 POPE/POPG) or 10 Å (90:28 POPG) of LeuT, immersed in a solution of explicit waters, ions, and randomly dispersed monomeric DDM detergents. In the second set of simulations ("Resulting Configurations"), LeuT retains only its core of lipids (10, 25, or 50 lipids) chosen from the representative snapshot from "Starting Configuration" trajectories. The core LeuT/lipid complexes were surrounded by a randomly placed monomeric detergent (either DDM or MNG-3) and lipids as required to create the stated simulation conditions, and the new MD simulations were performed for the time durations marked in the respective boxes.

that is appropriate for the experiment being performed. Nevertheless, high-resolution structural studies of various membrane proteins that rely on the solubilization step have revealed annular lipid components (i.e., lipids bound to the membrane-embedded regions of the protein) tightly bound to the protein,[3−8] which were presumably retained during the transfer of the protein from the native lipid bilayer to the detergent environment. This is of great interest because recent findings from *in vitro* assays of membrane protein function have shown that experimental conditions can strongly influence the functional behavior of proteomicelle systems,[9−12] implying a potential role of the annular lipids in the differential effects on protein structure and function under different preparatory protocols.

A pertinent example is LeuT, a bacterial homologue of the neurotransmitter:sodium symporter (NSS) family, which has served as a structural and functional prototype for the mammalian NSS homologues that are responsible for the re-uptake of neurotransmitters from the synaptic cleft into the presynaptic nerve terminal.[13,14] Substrate transport by NSS transporters is made possible by a coupling of the thermodynamically uphill uptake of substrate to the transmembrane Na^+ gradient.[15] In LeuT, computational and functional experiments[16] have identified a secondary high-affinity substrate binding site, termed the S2 site, located in the extracellular vestibule of LeuT, ∼11 Å above the central high-affinity primary substrate binding (S1) site discovered crystallographically.[17−19] In crystal structures, the extracellular vestibule has been shown to bind antidepressants,[20] and antidepressant binding inhibits substrate binding as well as transport. The two binding sites are proposed[16] to be allosterically connected in a mechanistic model of Na^+-coupled symport, whereby intracellular release of the S1-bound substrate is triggered by the binding of a second substrate molecule in the S2 site.

The existence of the LeuT S2 site was questioned because binding of substrate to the site had not been demonstrated crystallographically,[21] but subsequent studies revealed that treatment of LeuT with different concentrations of the detergent *n*-dodecyl β-D-maltopyranoside (DDM) during experimental preparations could account for the difference in the observed molar substrate (Leu) binding stoichiometry.[9] Thus, while at DDM concentrations below 0.15% (w/v), the Leu:protein binding stoichiometry was 2:1, at higher detergent concentrations [>0.175% (w/v)], only one Leu molecule is bound in a LeuT molecule, i.e., a molar binding stoichiometry of unity. Together with data collected from LeuT mutants with impaired S1 or S2 sites, these data suggest that binding of detergent results in the inability of LeuT to bind leucine in the S2 site. Interestingly, a substrate binding stoichiometry of 2:1 can be recovered by reconstituting LeuT that had been previously solubilized with high concentrations of DDM, into proteoliposomes composed of polar *Escherichia coli* lipids.[9] In addition, it has been shown that when LeuT is reconstituted into nanodiscs, the specific binding of both Leu and Ala (which also acts as a substrate for LeuT) is ∼1.5 times greater than in DDM,[22] and that another detergent, *n*-octyl β-D-glucopyranoside (OG), which has been found crystallographically to bind in the extracellular vestibule, may inhibit transport by preventing the substrate from accessing the S2 site.[23]

In a recent computational investigation of LeuT/DDM proteomicelles,[24] we found that at high DDM ratios the S2 site could be occluded by nontransient insertion of DDM, which

DOI: 10.1021/acs.biochem.5b01268
Biochemistry 2016, 55, 850−859

would sterically hinder the binding of substrate. Two distinct pathways for penetration of DDM into the LeuT S2 site were identified in these extensive unbiased atomistic molecular dynamics (MD) simulations of LeuT in a DDM proteomicelle. Once inserted, DDM was observed to engage in stable interactions with functionally important residues in the S2 site, such as Arg30, Gln34, Asp404, Phe320, and Leu400. Furthermore, the simulations established quantitatively the protein:DDM (P:D) number ratios at which such detergent penetration occurs: at P:D ratios of ∼1:246 or higher, DDM molecules would nontransiently insert into the S2 site, whereas at lower compositions, DDM penetration should be transient at most.

Because annular lipids are retained during the protein solubilization process, the computational investigations conducted in the absence of lipid had to be expanded to address the mechanistic role of the lipids surrounding the protein. It is expected that when detergent concentrations increase, the majority of (weakly) bound lipids are displaced, whereas the annular lipids tightly bound to specific protein regions could remain. In the case of detergent penetration, we previously observed that the long-lasting binding to the S2 site required penetration from a region that is expected to be in contact with the membrane. Thus, it is possible that the presence of tightly bound annular lipids could preserve the functionality of the S2 site even in the presence of detergent. This raises the question of the conditions and the size of the lipid annulus that are sufficient to preserve this functionality in a protein being solubilized in detergent.

In the context of the hypothesis originating from our earlier experimental work[2] that attributes the impairment of the S2 site to DDM penetration, it is possible to establish criteria for the appropriate concentrations of lipid and detergent that will maintain LeuT function and in particular S2 binding. To this end, we have followed up on our previous computational studies of LeuT/DDM proteomicelles[24] with extensive atomistic MD simulations of LeuT in the mixed environment of phospholipid and detergent molecules, including DDM and lauryl maltose-neopentyl glycol (MNG-3). By systematically varying relative lipid:detergent number ratios around LeuT (see Figure 1), we analyzed the results of the computational simulations in terms of the configurations and contents of a LeuT proteomicelle along the transporter solubilization process. The findings from our computational analysis are interpreted in the context of experimental ligand binding assays and suggest a crucial role of annular lipids in the experimentally measured binding function of LeuT.

MATERIALS AND METHODS

Molecular Dynamics Simulations. *Molecular Constructs.* To study LeuT in a mixed lipid/detergent environment with atomistic MD simulations, we made use of previously published[25] long atomic MD simulations of LeuT in a membrane composed of 23% 1-palmitoyl-2-oleoyl-*sn*-glycero-3-phosphoglycerol (POPG) and 77% 1-palmitoyl-2-oleoyl-*sn*-glycero-3-phosphoethanolamine (POPE) lipids, and extracted a representative snapshot from this MD trajectory of the LeuT with its surrounding shell of lipids. The LeuT model was the same as the one used in earlier LeuT simulations in DDM micelles[24] and was based on the X-ray structure from Protein Data Bank entry 3GJD.[23] In this structure, the transporter is in the occluded state and contains leucine (Leu) in the S1 site and two Na^+ ions in sites termed Na1 and Na2. The detergent *n*-octyl β-D-glucopyranoside (OG) in the S2 binding site of the 3GJD model was removed prior to the simulations. As detailed previously,[24] the residues missing from the 3GJD structure were added with Modeler,[26] and Glu112, Glu287, and Glu419 were treated as protonated.[27,28]

To design the various initial conditions of lipid:detergent number ratios ("Starting Configurations" in Figure 1), LeuT was extracted from the snapshots (see above) together with the lipids that had one heavy atom within either 5 or 10 Å of the transporter. The two lipid annuli extracted in this manner contained 53 POPEs and 19 POPGs or 90 POPEs and 28 POPGs, respectively (Figure 1). These LeuT/lipid complexes were then placed in a cubic box with a volume of ∼182^3 $Å^3$ and were surrounded by a dispersion of DDM detergent molecules positioned randomly in the solution as monomers so that the resulting DDM concentration of 0.08 M [or 4% (w/v), corresponding to 307 DDM detergents in the simulation box after the removal of overlapping detergent molecules] was well above the established critical micelle concentration (CMC) for DDM (170 μM).[29,30] The overall number of atoms in the simulation box after solvation with a 0.15 M Na^+Cl^- ionic solution was ∼518000.

As detailed in Results, the initial set of MD simulations converged after >300 ns to configurations with similar lipid shells (defined by the lipids within 4 Å of the protein), containing 35−40 POPEs and 10−15 POPGs (Figure 1). Guided by these shell sizes, the simulations in the next set were designed ("Resulting Configurations" in Figure 1) from the representative snapshots of the "Starting Configurations" simulations, with LeuT extracted with lipid annuli of various sizes [10, 25, or 50 lipids in the shell (see Figures 1 and also Results)], and surrounded with either DDM (307 molecules) or MNG-3 [160 molecules corresponding to a concentration of 0.04 M or 4% (w/v)]. We note that because the CMC of MNG-3 (10 μM) is significantly lower than that of DDM, the chosen number of detergent molecules (for similar simulation cell dimensions) ensured that LeuT was simulated in the regime of high detergent concentration relative to CMC for both DDM and MNG-3.

To evaluate the penetration of detergent into LeuT in MNG-3 proteomicelles, we also simulated LeuT in an MNG-3 environment in the absence of phospholipids (Figure 1). To this end, we designed a micelle around LeuT containing 160 MNG-3 molecules with the packing optimization program Packmol.[31] Packmol utilizes an optimization algorithm to generate a molecular system according to constraints set by the user and avoiding atomic overlaps. The system was first centered on the center of mass of LeuT and aligned to LeuT's principal axes. Several geometric constraints were then provided to Packmol for the design of the LeuT/MNG-3 proteomicelle: (i) the terminal carbons of one of the MNG-3 alkane chains (see Figure S1 of the Supporting Information) were constrained to lie within a central sphere with a 40 Å radius, and outside a cylinder, oriented by the principal axes, with a height of 100 Å and a radius of 20 Å; (ii) the ring oxygen of the second glucose moiety of MNG-3 was constrained to be outside a sphere with a radius of 50 Å and between two planes defined as +30 and −30 Å in the *z* plane (*z* being the direction along LeuT's axis that is perpendicular to the membrane). In this manner, in the resulting LeuT/MNG-3 proteomicelle, the detergent tails were appropriately placed to cover the hydrophobic core of LeuT while leaving hydrophilic regions of the protein exposed to the solvent.

Force Fields and MD Simulation Parameters. The atomistic MD simulations were conducted with the NAMD 2.9 package[32]

DOI: 10.1021/acs.biochem.5b01268
Biochemistry 2016, 55, 850−859

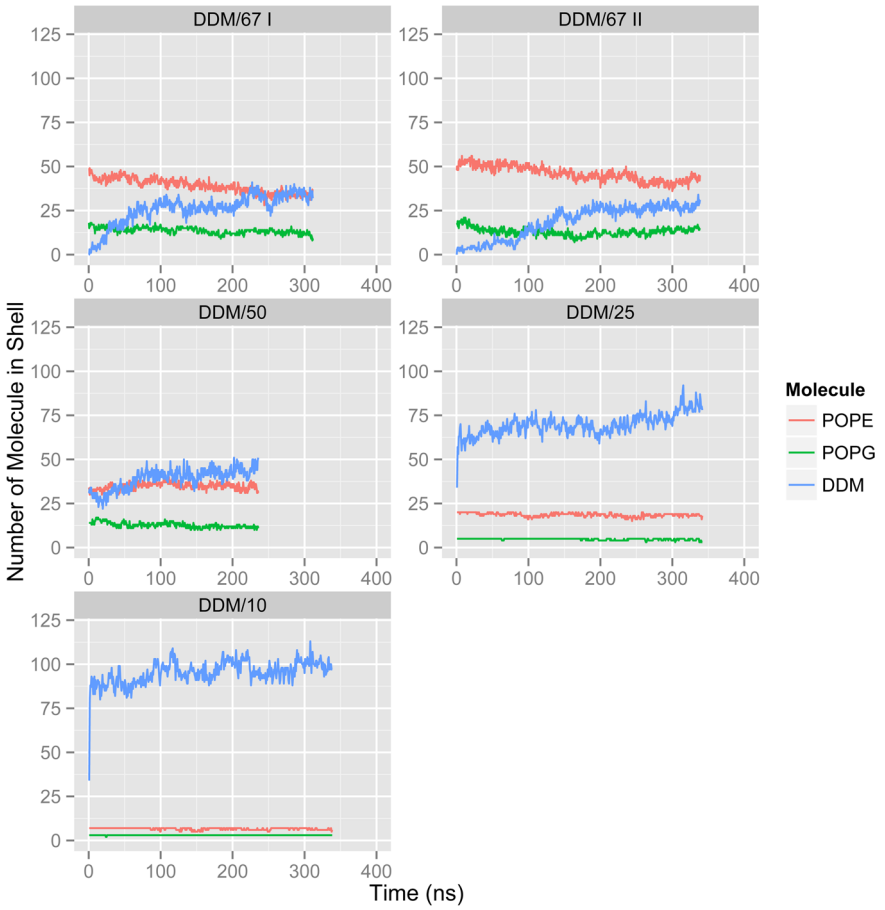

Figure 2. Time evolution (after initial equilibration phase) of the number of POPE (red), POPG (green), and DDM (blue) molecules within 4 Å of protein (i.e., shell) in different simulations from Figure 1.

using the all-atom CHARMM27 force field with CMAP corrections for proteins,[33] the CHARMM36 force field for lipids,[34] and a CHARMM-compatible force field parameter set for detergents.[35] CHARMM-suitable force field parameters for the MNG-3 molecule (provided in the Supporting Information) were generated with MATCH[36] using the top_all36_cgenff force field option and a 3D structure file for MNG-3 created with the Schrodinger software package Maestro (version 9.3, Schrödinger, LLC, New York, NY). Inspection of the resulting parameter set for MNG-3 from MATCH confirmed that all structural segments of the MNG-3 molecule shared with DDM were parametrized with MATCH in a manner identical to that expected from CHARMM-based force fields. All the molecular constructs were equilibrated and subjected to long production MD runs (see Figure 1 for details on simulation times) following the protocols and simulation parameters described in our earlier work on LeuT/DDM proteomicelles.[24]

Protein Expression, Purification, and Preparation for Functional Assays. LeuT was produced in *E. coli* C41(DE3) from plasmid pQO18, which encodes an N-terminally 10-His tagged recombinant version of the protein.[16,37] Protein was extracted from the membrane and purified by immobilized metal (Ni^{2+}) affinity chromatography in the presence of DDM.[3] Exchange of DDM with MNG-3 was achieved with high-performance liquid chromatography-mediated size-exclusion chromatography (Shodex Protein-KW803 column) in a buffer composed of 150 mM Tris/Mes (pH 7.5), 50 mM NaCl, 1 mM TCEP, 10% (w/v) glycerol, and 0.01% (w/v) (0.1 mM) MNG-3.

Binding Studies. Binding of 100 nM [^{3}H]Leu (140 Ci/mmol; American Radiolabeled Chemicals, Inc.) was measured by means of the scintillation proximity assay (SPA).[37] Prior to measuring the time course of binding of [^{3}H]leucine to 0.8 pmol of purified LeuT per assay, we incubated protein in either 0.1% DDM or 0.01% MNG-3 for 3 h at 23 °C in 150 mM Tris/Mes (pH 7.5), 50 mM NaCl, 1 mM TCEP, and 20% glycerol with DDM or MNG-3 at the indicated concentration. The time course of [^{3}H]Leu binding was monitored by measuring counts per minute in a Wallac photomultiplier tube MicroBeta microplate counter in SPA mode; 800 mM imidazole was added to a set of samples for each condition to determine the nonproximity cpm, which were subtracted from the total cpm (in the absence of imidazole) to obtain the specific cpm. Protein was assayed prior to binding experiments.[38] All experiments were repeated at least in duplicate, and data points show the mean ± the standard error of the mean (SEM) of triplicate determinations of representative experiments.

RESULTS

Stages of LeuT Solubilization in DDM Detergent Characterized via MD Simulations. To investigate the effects of annular lipids on the organization and dynamics of proteomicelles that form during LeuT solubilization, it is desirable to follow the detergent-mediated transition of LeuT from the initial complex with the native lipid membrane into a proteomicelle that may still contain residual lipids bound to LeuT. The protocol we adopted for this purpose is designed to

DOI: 10.1021/acs.biochem.5b01268
Biochemistry 2016, 55, 850−859

overcome the difficulties encountered by both experiment and simulation. Thus, characterization of the molecular details of the transition of LeuT between the environments is not feasible experimentally, while the time scale of the solubilization process exceeds the capability of unbiased molecular dynamics simulations. Therefore, we constructed atomistic models of LeuT in a mixed lipid/detergent environment that define configurations of the evolving LeuT proteomicelle along the solubilization pathway (see Materials and Methods for details) and followed the dynamics of these intermediate models with extensive MD simulations. The protocol starts with a construct of LeuT with its annulus of lipids extracted as described in Materials and Methods from our recently published[25] MD trajectories of LeuT in 77:23 POPE/POPG membranes. Two different sizes of lipid annuli were extracted, containing phospholipids residing within 5 or 10 Å of LeuT in the bilayer simulation trajectory. The complete starting system consisted of these LeuT/lipid complexes immersed in a solution containing randomly dispersed monomeric DDM molecules (see Materials and Methods). The MD simulation trajectories were obtained for >300 ns (simulations DDM/67 I and II in Figure 1).

Annular Lipids in LeuT Proteomicelles. Our previous computational work on LeuT in DDM micelles[24] established the importance of the size of the micelle surrounding the protein in determining the effect of the detergent. The results showed that although the overall number of molecules in the proteomicelle depends on concentration, the number of DDM molecules in the 4 Å shell surrounding the protein is independent of the overall DDM concentration. This organization is stabilized relatively fast in the simulations (~100−150 ns). Indeed, as shown in Figure 2, the two trajectories (DDM/67 I and II, which contain DDM, POPE, and POPG molecules in the LeuT shell) converged to configurations with very similar core measures within 100−150 ns: ~30−35 DDMs, ~35−40 POPEs, and ~12−15 POPGs. Importantly, the time profiles for the evolution of DDM/67 I and II, shown in Figure 2, indicate a gradual displacement of lipids from the protein core by detergent molecules, i.e., a dynamic transformation that takes place during the protein solubilization process. In this process, detergent molecules are seen to eventually replace all but a few structural lipids that are most tightly packed around the protein. The simulation also tracked the formation of separate aggregates that were not part of the central proteomicelle and contained mixtures of lipid surrounded by detergent. Thus, both free aggregates (FA) and free monomers (FM) were found in the solution containing the proteomicelle (see Figure 3), similar to results obtained previously in the absence of lipid, and in agreement with the expected physicochemical process of solubilization.

The regions of the transporter engaged in interactions with the structural nucleus of lipids strongly bound to LeuT were investigated in the DDM/67 I and DDM/67 II trajectories. The average numbers of POPE, POPG, and DDM molecules with at least one atom within 3 Å of each residue were calculated, and Figure 4 shows the resulting density maps for the lipid and detergent components as a function of protein sequence. The results in Figure 4 identify specific segments in LeuT that make frequent contacts with lipid/detergent molecules and specify sites that show a preference for either POPE or POPG lipids. Because the fatty acid chains of POPE and POPG are identical, the selectivity for the various TM surfaces of LeuT is most likely the result of interactions between the side chains of the protein residues and lipid headgroups, although it may also involve alternative packing of the lipids induced by lipid−lipid

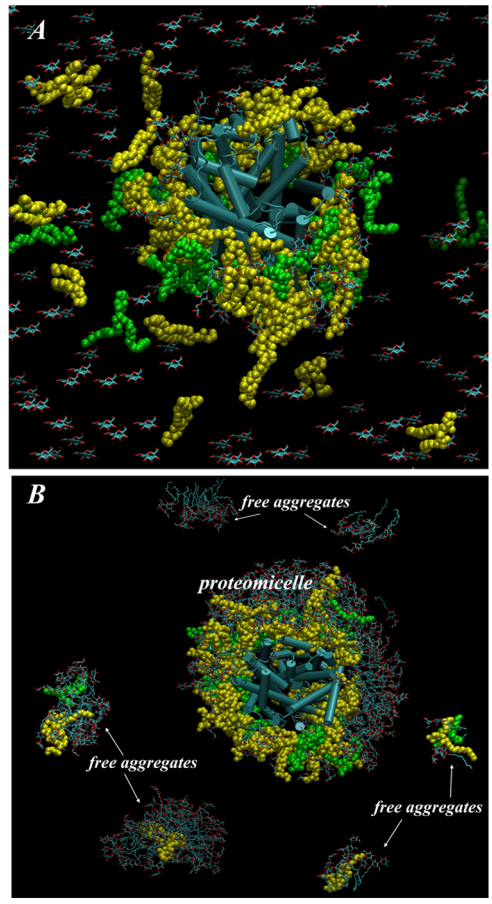

Figure 3. LeuT in a mixed lipid/detergent environment: the centrally located proteomicelle and free aggregates in the solution. Initial configuration (A) and final snapshot (B), after 194 ns MD simulations, of LeuT (cartoon) surrounded by 53 POPE lipids (yellow color), 19 POPG lipids (green color), and 307 DDM detergent molecules (cyan color) (from simulation DDM/50 in Figure 1). For the sake of clarity, water molecules, ions, and transporter-bound Leu were omitted from the snapshots.

headgroup interactions. Interestingly, the TM6/TM11 interface displays more significant penetration by detergent in DDM/67 I (constructed from the 5 Å lipid shell) than in DDM/67 II (constructed from the 10 Å lipid shell). Previously, we found this interface to constitute the pathway through which DDM penetrated LeuT to make long-lived contacts in S2.[24]

The observed lipid binding specificity was then used in the construction of systems designed to investigate the effect of lipid cores on the penetration of DDM into the S2 site. The protocol for the definition of the lipid cores was used to obtain three different starting systems for subsequent MD simulation in the presence of detergent: a "small core", a "medium core", and a "large core" were obtained on the basis of the results in Figure 4. To create these cores, the residues with the largest average number of interacting lipids were identified. For example, in the DDM/67 I trajectory, Ile48, Ile292, and Phe496 were found to interact most frequently with POPE and Arg88, Phe177, and Leu380 with POPG. The lipids that bound to these six residues were extracted from a representative snapshot of the DDM/67 I trajectory and used as a 10-lipid core (seven POPEs and three POPGs) designated as the "small core" (see Figure 5A). The same procedure was used to define the "medium core" of 25 lipids (20 POPEs and 5 POPGs) around the top 12 lipid-

DOI: 10.1021/acs.biochem.5b01268
Biochemistry 2016, 55, 850−859

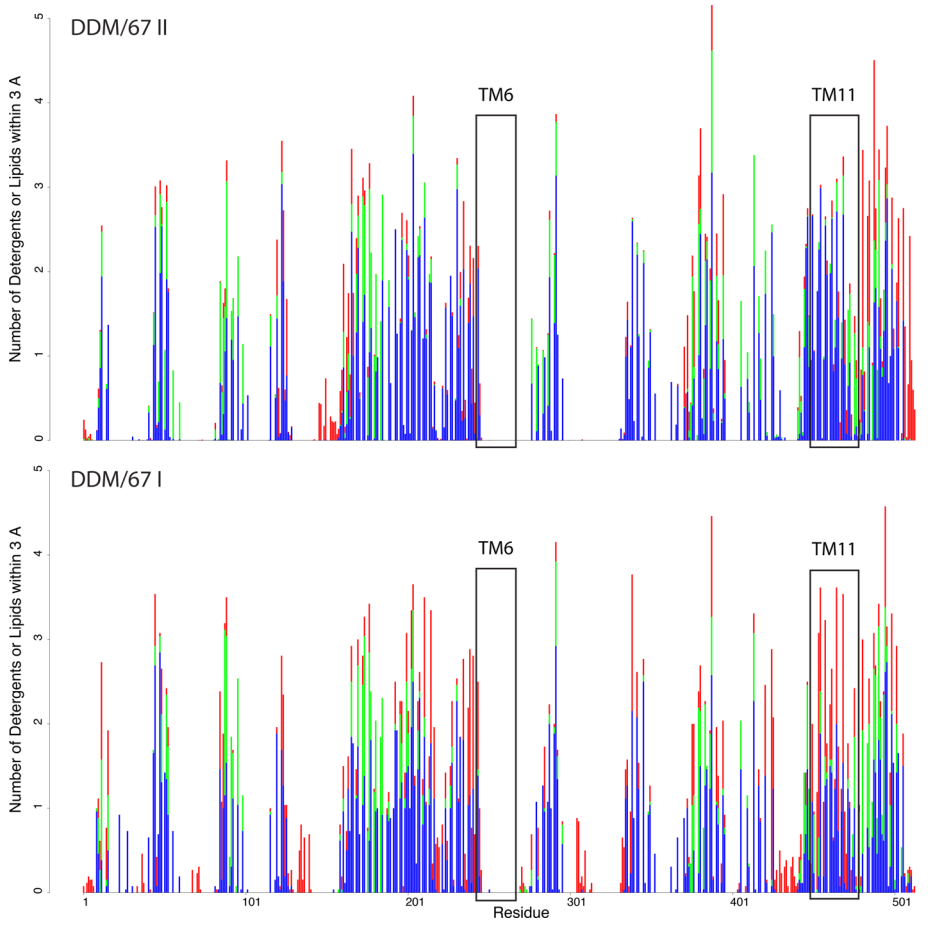

Figure 4. Average number of lipid or detergent molecules contacting LeuT as a function of residue number. The average number of detergent or lipids with 3 Å of LeuT for each residue in the DDM/67 I (bottom) and II (top) simulations. Each bar stacks the average number of contacts from POPE (blue), POPG (green), and DDM (red). Black boxes are included to indicate TM6 and TM11.

interacting residues, which additionally included Ile45, Ile174, Il184, Phe388, Phe494, and Leu495 (Figure 5B).

For MD simulations, the LeuT models with small and medium cores were surrounded by DDM detergents in the same formation that is found in the trajectory frames from which the cores were extracted, and the new MD simulations were termed DDM/10 and DDM/25 (Figure 1).

Finally, we simulated a "large core" of 50 lipids (35 POPEs and 15 POPGs) to see how detergent competition with annular lipids may be affected by the presence of additional competing lipids in solution. This larger core was therefore generated from the DDM/67 I trajectory, and it contained all lipids within 4 Å of any residue of the transporter after 312 ns. For the simulation, this LeuT/lipid core complex was immersed in solution containing randomly dispersed monomeric DDM, POPE, and POPG molecules, and the entire system was used as the initial configuration of the DDM/50 simulation (Figure 1).

On the basis of this design, the three LeuT/lipid core constructs (with small, medium, and large cores) provided the initial molecular models for mixed lipid/detergent environments surrounding LeuT at various stages of the protein solubilization process. Indeed, the DDM/25 and DDM/50 simulations showed a small degree of gradual replacement of the core lipids with the detergent (Figure 2), whereas all the lipids in the DDM/10 system remained LeuT-bound on the simulation time scales. Importantly, the analysis of the trajectories for DDM/10 and DDM/25 was consistent with the DDM/67 I and II simulations, in which DDM extensively penetrated into the TM6/TM11 interface.

Lipids from the LeuT Proteomicelle Shell and DDM Molecules from the Solution Exchange at a Ratio of 2:1. Figure 2 compares compositions of the LeuT cores in the simulations initiated from different size annuli of lipids around the protein. It reveals the delicate interplay between the lipid and detergent molecule numbers in the transporter core at different stages of solubilization. Specifically, in the course of the simulations, the small size lipid core (DDM/10) is penetrated by ~100 DDM molecules, whereas the medium (DDM/25) and large (DDM/50) lipid cores attract ~70 and ~40 detergent molecules, respectively. In comparison to the LeuT/DDM proteomicelles reported previously,[24] we find here that the shell DDM numbers equilibrate at 120 ± 7 irrespective of the overall protein:detergent number ratio. Thus, in the context of the detergent-mediated solubilization transition, the calculated core measures suggest that on average approximately two DDM molecules replace each lipid molecule extracted from the LeuT shell. Because interactions of the transporter with its lipid annulus are mostly driven by hydrophobic/hydrophilic effects that shield hydrophobic TMs of LeuT from unfavorable polar exposure, the equivalency of the core numbers between different simulations demonstrates that the effective volume occupied by a single lipid molecule in the core is roughly twice that taken by a DDM detergent molecule.

DOI: 10.1021/acs.biochem.5b01268
Biochemistry 2016, 55, 850−859

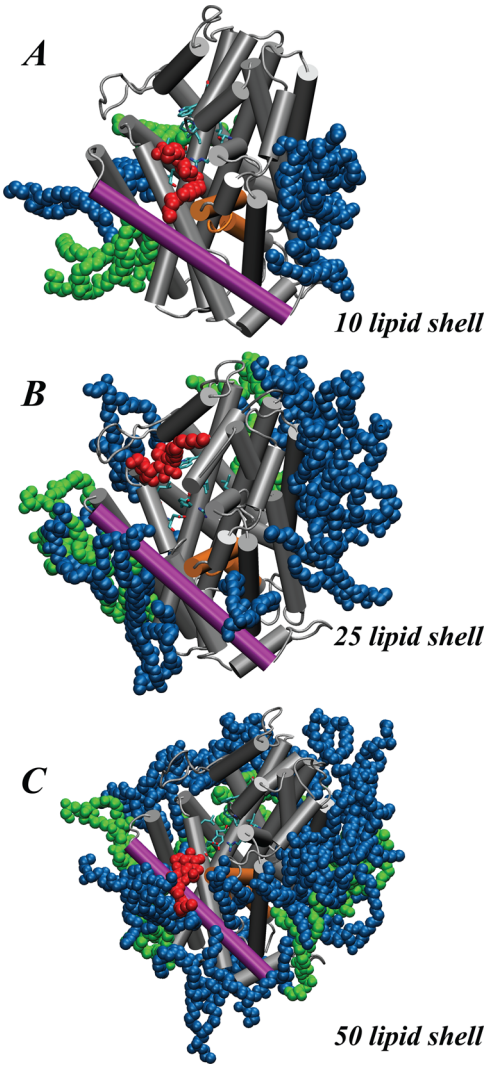

Figure 5. Lipid shells of different sizes around LeuT. Final snapshots of small (A), medium (B), and large (C) size lipid cores around LeuT (see also Figure 1). POPE, POPG, and the closest DDM to the S2 site are colored blue, green, and red, respectively; the protein is depicted as a cartoon. S2 residues are shown as licorice, and TM6 and TM11 of LeuT are colored orange and purple, respectively.

Annular Lipids Protect LeuT from DDM Penetration in the S2 Site. In the DDM/67 I and II trajectories, we observed some transient penetrations of LeuT by DDM, but the detergent molecule did not insert completely. In the DDM/50 simulation (see Figure 6, labeled by simulation), any such DDM molecules penetrating transiently in the beginning stages of the simulation were rapidly replaced by a lipid molecule. In the pure DDM proteomicelles,[24] we had observed two modes of DDM penetration: one in which the DDM approached the S2 site from the extracellular domain ("from the top"), making interactions with Phe320 of ECL4 and Leu400 of TM10, and another in which the DDM approached "from the side", inserting into LeuT from the area between the extracellular ends of TM11 and TM6 and making long-lasting contacts with Asp404, Gln34, and Arg30. Here, in the presence of lipid cores, the movement of DDM into LeuT is always "from the side" and is reasonably attributable to the absence of strongly bound lipids near the extracellular TM11/TM6 interface. In the simulations with medium and small lipid cores, this entrance is completely exposed initially, and it remains exposed (see Figure 5A,B). However, when the lipid:DDM ratio is high, lipids prevent complete entry "from the side"; as the concentration of detergent increases and outcompetes the annular lipids, detergent entry becomes possible. While some "from the top" interaction between detergents and the Phe320 and Leu400 residues was seen in the medium shell simulation (see Figure 5B), the penetration was not complete. Indeed, the only simulation in which complete penetration of a DDM into the LeuT S2 site was observed is with the small lipid shell simulation (see Figure 5A). Notably, the protein:detergent ratio in our present simulations is far above ratios at which we had already observed long-lived penetration in our previous simulations in pure DDM (<1:240),[24] making it clear that the presence of annular lipid prevents penetration of DDM "from the side" in all but the smallest lipid shell system.

MNG-3 Detergent Molecules Do Not Penetrate the S2 Site. As the annular lipids prevent DDM penetration by competing for occupancy of the TM11/TM6 interface that allows access to the S2 site, we hypothesized that larger detergent molecules with volumes comparable to those of the lipids would not be able to fit into the interface and would not penetrate into the S2 site. To probe this hypothesis computationally, we constructed simulations of LeuT in a mixed lipid/detergent environment with the amphiphile detergent MNG-3 (see Materials and Methods), which is known to better stabilize TM proteins, including LeuT.[39] As the MNG-3 structure is composed of two DDM molecules that share a common carbon at the second position of the alkyl chains (Figure S1), it is reasonable to assume that the effective volume occupied by a single MNG-3 molecule will be larger than that of DDM when packed into the proteomicelle.

In the simulations of mixed lipid/MNG-3 environments at various lipid:detergent ratios (see Figure 1), we find that MNG-3 is gradually assimilated into the proteomicelle, similar to what we observed for DDM (see Figure S2). Still, MNG-3 does not penetrate into the S2 site, independent of the quantity of lipids in the core (see Figure S3). Given that the CMC of DDM is an order of magnitude greater than that of MNG-3 (see Materials and Methods), our simulations in MNG-3 correspond to conditions of detergent concentration far greater than those required to solubilize LeuT and sufficiently high to see penetration if it were possible.

Because our results suggest that MNG-3 does not penetrate into the S2 site, we hypothesized that MNG-3 would not compete with leucine for binding to the S2 site as has been previously observed for DDM.[9] To test this hypothesis, we performed leucine binding using the SPA (see Materials and Methods) with various concentrations of DDM and MNG-3 (see Figure 7). As expected from our previous experiments and simulations, the level of leucine binding is reduced to ~50% when the DDM concentration is increased from 0.1 to 0.3%. However, binding of [^{3}H]Leu in the presence of increasing concentrations of MNG-3 was virtually identical to that observed in the presence of 0.1% DDM, a condition that maintained a 2:1 binding stoichiometry.[9]

DISCUSSION

Membrane protein solubilization in detergent is an essential step in the experimental protocol that allows structural and functional experiments to be conducted with various polytopic membrane proteins such as LeuT. It has always been known to have potential deleterious effects on protein stability,[40] but to the best

DOI: 10.1021/acs.biochem.5b01268
Biochemistry 2016, 55, 850−859

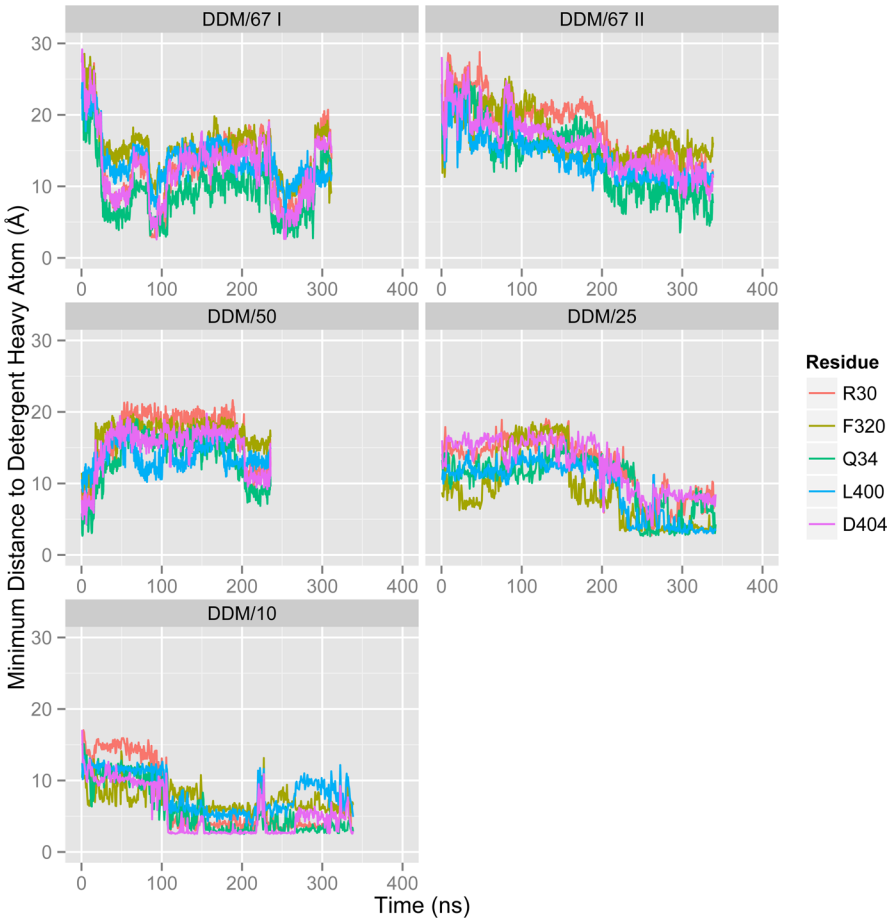

Figure 6. DDM binding in the S2 site. Minimum distance from S2 site residues (R30, F320, Q34, L400, and D404) to the heavy atoms of the nearest DDM detergent molecule as a function of time in various MD trajectories.

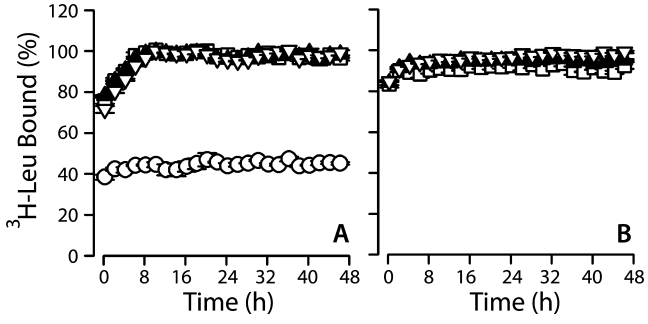

Figure 7. Effect of detergent on LeuT binding activity. Time course of binding of 100 nM [^{3}H]Leu to 0.8 pmol of LeuT assayed with the SPA with (A) protein prepared in 0.1% DDM or (B) protein that was subjected to detergent exchange from DDM to MNG-3 by size-exclusion chromatography. In panel A, increasing concentrations of MNG-3 [0.1% (▲) and 0.5% (▽)] were added to protein in 0.1% DDM (□). In addition, binding of 100 nM [^{3}H]Leu to LeuT in the presence of 0.3% DDM (○) was measured.[4] In panel B, increasing concentrations of MNG-3 were added to the sample prepared (after exchange) in 0.01% MNG-3 (□) to yield final concentrations of 0.1% (▲) and 0.5% (▽). Data points are the mean ± SEM of triplicate determinations of a representative experiment and are normalized to the activity of binding in the presence of 0.1% DDM.

of our knowledge, the fact that many traditional measures of stability can be maintained in the face of functional artifacts is not as widely appreciated. This requires a mechanistic understanding, and therefore, we conducted the extensive MD simulations of LeuT in mixed lipid/detergent proteomicelles consisting of different concentrations of lipid and two different detergent molecules presented here. These simulations have explored conditions that can create such artifacts in one system and corroborated the mechanism identified previously for the occlusion by DDM of the secondary substrate (S2) site in LeuT. The simulated constructs of the LeuT protein surrounded by lipid cores of different sizes immersed in detergent environments provided the initial molecular models for the analysis of dynamics in mixed lipid/detergent environments at various stages of the protein solubilization process. The results of the simulations offer mechanistic insights into the role of the concentration and chemical nature of detergent on the experimental measurements of function in the presence of annular lipids. We find that as LeuT becomes solubilized by DDM, the detergent molecules gradually outcompete lipids and eventually, at sufficiently low lipid:detergent ratios, start to penetrate into the S2 site. Mechanistically, it becomes clear from the simulations that the least preferred region of lipid−protein interaction in LeuT is the TM6/TM11 interface, which is particularly vulnerable to penetration by DDM when it becomes possible at the low lipid:DDM ratios. Through experimental probing of the various conditions, we find that at high DDM (but not MNG-3) concentrations, the level of binding of Leu to LeuT is reduced ~2-fold, which is indicative of a reduction of the binding stoichiometry from 2:1 to 1:1.[9] On the basis of the molecular-level insights provided by the simulations in the presence of lipid, we propose that the stoichiometry remains 2:1 even at the highest MNG-3 concentrations studied

DOI: 10.1021/acs.biochem.5b01268
Biochemistry 2016, 55, 850−859

here because MNG-3 cannot penetrate into the S2 site. We reason that its bulky tails, which are similar to those of the lipids we studied in the lipid/detergent mixed systems, allow it to protect the TM6/TM11 interface. It should be noted that the simulations presented here and previously[24] do not inform whether this mechanism is kinetic or thermodynamic in nature but do indicate that it is likely competitive. A differentiation between the two possible mechanisms could be achieved in the future from specific experiments and additional simulations.

In addition to their obvious significance for understanding the potential artifacts associated with protein solubilization in detergents, the results presented here underscore yet another aspect of the involvement of the lipid environment in membrane protein function. Thus, various mechanisms have been documented for the influence of membrane lipid composition on the function of membrane proteins (including modulation due to changes in the membrane mechanical properties and local deformations that affect the energetics of hydrophobic mismatch[25,41−43]). Here we document an additional mechanism in which the lipids protect the integrity of a protein's binding functionality from penetration by other molecules. It is likely that in the cellular environment local to LeuT, for example, the ratio of lipids to small molecules that could potentially bind nonspecifically to the S2 site is high, and thus, there is a low likelihood of penetration of these molecules into the S2 site in the "from the side" manner, preventing unanticipated inhibition by nonsubstrates. However, when the protein is studied in a nonphysiological environment, such as in the highly concentrated detergent solutions used in many experiments, functional sites of LeuT may become exposed to the detergent because residual amounts of lipids carried over from the purification step are not sufficient to protect these functional sites. This effect could be especially important in systems that are suggested to bind hydrophobic ligands that enter from the membrane, such as the ligands for the cannabinoid,[44] κ-opioid,[45] and rhodopsin[46] G-protein-coupled receptors (GPCRs). When a permeation path from the membrane into a binding site exists for functional purposes, it may be essential that the annular lipids in that region be maintained in *in vitro* experiments.

In conclusion, our results reveal specific mechanistic reasons for the particular care that must be taken when choosing the appropriate detergent molecules and their concentrations for solubilization. The functional role of the S2 site in the mechanism of transport of LeuT has been a subject of debate, and our recent computational and experimental findings suggest that much of the controversy can be explained by differences in experimental conditions. An increased level of attention to the effect of experimental conditions on measurements of function not only will reduce the likelihood that controversies arise due to artifacts but also may lead to improved insights into the role of these agents in protein function and especially in analyzing the manner in which the direction and stoichiometry of binding of ligand to membrane proteins can be affected.

■ ASSOCIATED CONTENT

Supporting Information

The Supporting Information is available free of charge on the ACS Publications website at DOI: 10.1021/acs.biochem.5b01268.

Additional figures (PDF)

■ AUTHOR INFORMATION

Corresponding Author

*Department of Physiology and Biophysics, WCMC, 1300 York Ave., Room LC-501A, New York, NY 10065. E-mail: gek2009@med.cornell.edu. Phone: 212-746-6539. Fax: 212-746-6226.

Funding

This work was supported by National Institutes of Health (NIH) Grants DA022413, DA17293, P01 DA012408, and U54 GM087519 and by the Intramural Research Program of the NIH, National Institute on Drug Abuse (L.S.). M.V.L. is supported by Ruth L. Kirschstein National Research Service Award F31DA035533.

Notes

The authors declare no competing financial interest.

■ ACKNOWLEDGMENTS

The following computational resources are gratefully acknowledged: an XSEDE allocation at the Texas Advanced Computing Center at The University of Texas at Austin (Stampede supercomputer, Projects TG-MCB090132 and TG-MCB120008), an allocation at the National Energy Research Scientific Computing Center (NERSC, repository m1710, used for initial studies) supported by the Office of Science of the U.S. Department of Energy under Contract DE-AC02-05CH11231, and the computational resources of the David A. Cofrin Center for Biomedical Information in the HRH Prince Alwaleed Bin Talal Bin Abdulaziz Alsaud Institute for Computational Biomedicine.

■ ABBREVIATIONS

LeuT, leucine transporter; DDM, *n*-dodecyl β-D-maltopyranoside; MD, molecular dynamics; MNG-3, lauryl maltose-neopentyl glycol; NSS, neurotransmitter:sodium symporter; OG, *n*-octyl β-D-glucopyranoside; POPG, 1-palmitoyl-2-oleoyl-*sn*-glycero-3-phosphoglycerol; POPE, 1-palmitoyl-2-oleoyl-*sn*-glycero-3-phosphoethanolamine; CMC, critical micelle concentration.

■ REFERENCES

(1) Seddon, A. M., Curnow, P., and Booth, P. J. (2004) Membrane proteins, lipids and detergents: not just a soap opera. *Biochim. Biophys. Acta, Biomembr. 1666*, 105−117.

(2) Lichtenberg, D., Opatowski, E., and Kozlov, M. M. (2000) Phase boundaries in mixtures of membrane-forming amphiphiles and micelle-forming amphiphiles. *Biochim. Biophys. Acta, Biomembr. 1508*, 1−19.

(3) Kuhn, P., Choi, H.-J., Kobilka, B. K., Rasmussen, S. G. F., Cherezov, V., Stevens, R. C., Weis, W. I., Kobilka, T. S., Thian, F. S., Hanson, M. a, and Rosenbaum, D. M. (2007) High-Resolution Crystal Structure of an Engineered Human 2-Adrenergic G Protein Coupled Receptor. *Science 318*, 1258−1265.

(4) Liu, W., Chun, E., Thompson, A. a, Chubukov, P., Xu, F., Katritch, V., Han, G. W., Roth, C. B., Heitman, L. H., IJzerman, A. P., Cherezov, V., and Stevens, R. C. (2012) Structural basis for allosteric regulation of GPCRs by sodium ions. *Science 337*, 232−236.

(5) Laganowsky, A., Reading, E., Allison, T. M., Ulmschneider, M. B., Degiacomi, M. T., Baldwin, A. J., and Robinson, C. V. (2014) Membrane proteins bind lipids selectively to modulate their structure and function. *Nature 510*, 172−175.

(6) Koshy, C., Schweikhard, E. S., Gärtner, R. M., Perez, C., Yildiz, O., and Ziegler, C. (2013) Structural evidence for functional lipid interactions in the betaine transporter BetP. *EMBO J. 32*, 3096−3105.

(7) Penmatsa, A., Wang, K. H., and Gouaux, E. (2013) X-ray structure of dopamine transporter elucidates antidepressant mechanism. *Nature 503*, 85−90.

DOI: 10.1021/acs.biochem.5b01268
Biochemistry 2016, 55, 850−859

(8) McAuley, K. E., Fyfe, P. K., Ridge, J. P., Isaacs, N. W., Cogdell, R. J., and Jones, M. R. (1999) Structural details of an interaction between cardiolipin and an integral membrane protein. *Proc. Natl. Acad. Sci. U. S. A. 96*, 14706−14711.
(9) Quick, M., Shi, L., Zehnpfennig, B., Weinstein, H., and Javitch, J. A. (2012) Experimental conditions can obscure the second high-affinity site in LeuT. *Nat. Struct. Mol. Biol. 19*, 207−211.
(10) Dodes Traian, M. M., Cattoni, D. I., Levi, V., and González Flecha, F. L. (2012) A two-stage model for lipid modulation of the activity of integral membrane proteins. *PLoS One 7*, e39255.
(11) Amin, A., Hariharan, P., Chae, P. S., and Guan, L. (2015) Effect of Detergents on Galactoside Binding by Melibiose Permeases. *Biochemistry 54*, 5849−5855.
(12) Amin, A., Hariharan, P., Chae, P.-S., and Guan, L. (2015) Effect of Detergents on Galactoside Binding by Melibiose Permeases. *Biochemistry 54*, 5849−5855.
(13) Penmatsa, A., and Gouaux, E. (2014) How LeuT shapes our understanding of the mechanisms of sodium-coupled neurotransmitter transporters. *J. Physiol. 592*, 863−869.
(14) Loland, C. J. (2015) The use of LeuT as a model in elucidating binding sites for substrates and inhibitors in neurotransmitter transporters. *Biochim. Biophys. Acta, Gen. Subj. 1850*, 500−510.
(15) Gether, U., Andersen, P. H., Larsson, O. M., and Schousboe, A. (2006) Neurotransmitter transporters: molecular function of important drug targets. *Trends Pharmacol. Sci. 27*, 375−383.
(16) Shi, L., Quick, M., Zhao, Y., Weinstein, H., and Javitch, J. A. (2008) The mechanism of a neurotransmitter:sodium symporter−inward release of Na+ and substrate is triggered by substrate in a second binding site. *Mol. Cell 30*, 667−677.
(17) Yamashita, A., Singh, S. K., Kawate, T., Jin, Y., and Gouaux, E. (2005) Crystal structure of a bacterial homologue of Na+/Cl−dependent neurotransmitter transporters. *Nature 437*, 215−223.
(18) Wang, H., Goehring, A., Wang, K. H., Penmatsa, A., Ressler, R., and Gouaux, E. (2013) Structural basis for action by diverse antidepressants on biogenic amine transporters. *Nature 503*, 141−145.
(19) Wang, H., Elferich, J., and Gouaux, E. (2012) Structures of LeuT in bicelles define conformation and substrate binding in a membrane-like context. *Nat. Struct. Mol. Biol. 19*, 212−219.
(20) Zhou, Z., Zhen, J., Karpowich, N. K., Goetz, R. M., Law, C. J., Reith, M. E. a, and Wang, D.-N. (2007) LeuT-desipramine structure reveals how antidepressants block neurotransmitter reuptake. *Science 317*, 1390−1393.
(21) Piscitelli, C. L., Krishnamurthy, H., and Gouaux, E. (2010) Neurotransmitter/sodium symporter orthologue LeuT has a single high-affinity substrate site. *Nature 468*, 1129−1132.
(22) Nasr, M. L., and Singh, S. K. (2014) Radioligand binding to nanodisc-reconstituted membrane transporters assessed by the scintillation proximity assay. *Biochemistry 53*, 4−6.
(23) Quick, M., Winther, A.-M. L., Shi, L., Nissen, P., Weinstein, H., and Javitch, J. A. (2009) Binding of an octylglucoside detergent molecule in the second substrate (S2) site of LeuT establishes an inhibitor-bound conformation. *Proc. Natl. Acad. Sci. U. S. A. 106*, 5563−5568.
(24) Khelashvili, G., LeVine, M. V., Shi, L., Quick, M., Javitch, J. A., and Weinstein, H. (2013) The membrane protein LeuT in micellar systems: aggregation dynamics and detergent binding to the S2 site. *J. Am. Chem. Soc. 135*, 14266−14275.
(25) Mondal, S., Khelashvili, G., Shi, L., and Weinstein, H. (2013) The cost of living in the membrane: a case study of hydrophobic mismatch for the multi-segment protein LeuT. *Chem. Phys. Lipids 169*, 27−38.
(26) Sali, A., and Blundell, T. L. (1993) Comparative protein modelling by satisfaction of spatial restraints. *J. Mol. Biol. 234*, 779−815.
(27) Shaikh, S. A., and Tajkhorshid, E. (2010) Modeling and dynamics of the inward-facing state of a Na+/Cl- dependent neurotransmitter transporter homologue. *PLoS Comput. Biol. 6*, e1000905.
(28) Zhao, C., Stolzenberg, S., Gracia, L., Weinstein, H., Noskov, S., and Shi, L. (2012) Ion-controlled conformational dynamics in the outward-open transition from an occluded state of LeuT. *Biophys. J. 103*, 878−88.
(29) le Maire, M., Champeil, P., and Møller, J. V. (2000) Interaction of membrane proteins and lipids with solubilizing detergents. *Biochim. Biophys. Acta, Biomembr. 1508*, 86−111.
(30) Kaufmann, T. C., Engel, A., and Rémigy, H.-W. (2006) A novel method for detergent concentration determination. *Biophys. J. 90*, 310−317.
(31) Martínez, L., Andrade, R., Birgin, E. G., and Martínez, J. M. (2009) PACKMOL: a package for building initial configurations for molecular dynamics simulations. *J. Comput. Chem. 30*, 2157−2164.
(32) Phillips, J. C., Braun, R., Wang, W., Gumbart, J., Tajkhorshid, E., Villa, E., Chipot, C., Skeel, R. D., Kalé, L., and Schulten, K. (2005) Scalable molecular dynamics with NAMD. *J. Comput. Chem. 26*, 1781−1802.
(33) Brooks, B. R., Brooks, C. L., Mackerell, A. D., Nilsson, L., Petrella, R. J., Roux, B., Won, Y., Archontis, G., Bartels, C., Boresch, S., Caflisch, A., Caves, L., Cui, Q., Dinner, A. R., Feig, M., Fischer, S., Gao, J., Hodoscek, M., Im, W., Kuczera, K., Lazaridis, T., Ma, J., Ovchinnikov, V., Paci, E., Pastor, R. W., Post, C. B., Pu, J. Z., Schaefer, M., Tidor, B., Venable, R. M., Woodcock, H. L., Wu, X., Yang, W., York, D. M., and Karplus, M. (2009) CHARMM: the biomolecular simulation program. *J. Comput. Chem. 30*, 1545−1614.
(34) Pastor, R. W., and Mackerell, A. D. (2011) Development of the CHARMM Force Field for Lipids. *J. Phys. Chem. Lett. 2*, 1526−1532.
(35) Abel, S., Dupradeau, F.-Y., Raman, E. P., MacKerell, A. D., and Marchi, M. (2011) Molecular simulations of dodecyl-β-maltoside micelles in water: influence of the headgroup conformation and force field parameters. *J. Phys. Chem. B 115*, 487−499.
(36) Yesselman, J. D., Price, D. J., Knight, J. L., and Brooks, C. L. (2012) MATCH: an atom-typing toolset for molecular mechanics force fields. *J. Comput. Chem. 33*, 189−202.
(37) Quick, M., and Javitch, J. A. (2007) Monitoring the function of membrane transport proteins in detergent-solubilized form. *Proc. Natl. Acad. Sci. U. S. A. 104*, 3603−3608.
(38) Schaffner, W., and Weissmann, C. (1973) A rapid, sensitive, and specific method for the determination of protein in dilute solution. *Anal. Biochem. 56*, 502−514.
(39) Chae, P. S., Rasmussen, S. G. F., Rana, R. R., Gotfryd, K., Chandra, R., Goren, M. A., Kruse, A. C., Nurva, S., Loland, C. J., Pierre, Y., Drew, D., Popot, J., Picot, D., Fox, B. G., Guan, L., Gether, U., Byrne, B., Kobilka, B., and Gellman, S. H. (2010) Maltose−neopentyl glycol (MNG) amphiphiles for solubilization, stabilization and crystallization of membrane proteins. *Nat. Methods 7*, 1003−1008.
(40) Privé, G. G. (2007) Detergents for the stabilization and crystallization of membrane proteins. *Methods 41*, 388−397.
(41) Mondal, S., Khelashvili, G., Shan, J., Andersen, O. S., and Weinstein, H. (2011) Quantitative modeling of membrane deformations by multihelical membrane proteins: application to G-protein coupled receptors. *Biophys. J. 101*, 2092−2101.
(42) Mondal, S., Johnston, J. M., Wang, H., Khelashvili, G., Filizola, M., and Weinstein, H. (2013) Membrane driven spatial organization of GPCRs. *Sci. Rep. 3*, 2909.
(43) Mondal, S., Khelashvili, G., and Weinstein, H. (2014) Not Just an Oil Slick: How the Energetics of Protein-Membrane Interactions Impacts the Function and Organization of Transmembrane Proteins. *Biophys. J. 106*, 2305−2316.
(44) Hurst, D. P., Grossfield, A., Lynch, D. L., Feller, S., Romo, T. D., Gawrisch, K., Pitman, M. C., and Reggio, P. H. (2010) A lipid pathway for ligand binding is necessary for a cannabinoid G protein-coupled receptor. *J. Biol. Chem. 285*, 17954−17964.
(45) Khelashvili, G., Mondal, S., Andersen, O. S., and Weinstein, H. (2010) Cholesterol modulates the membrane effects and spatial organization of membrane-penetrating ligands for G-protein coupled receptors. *J. Phys. Chem. B 114*, 12046−12057.
(46) Park, J. H., Scheerer, P., Hofmann, K. P., Choe, H.-W., and Ernst, O. P. (2008) Crystal structure of the ligand-free G-protein-coupled receptor opsin. *Nature 454*, 183−187.

DOI: 10.1021/acs.biochem.5b01268
Biochemistry 2016, 55, 850−859